Journal of Nonlinear Optical Physics & Materials
Vol. 26, No. 4 (2017) 1750041 (10 pages)

DOI: 10.1142/S0218863517500412

World Scientific
www.worldscientific.com

Dynamically tailoring nonlinear Cherenkov radiation in PPLN by structured fundamental wave

Xiangling Fang, Haigang Liu, Xiaohui Zhao, Yuanlin Zheng and Xianfeng Chen*

State Key Laboratory of Advanced Optical Communication Systems and Networks, School of Physics and Astronomy, Shanghai Jiao Tong University, 800 Dongchuan Road, Shanghai 200240, P. R. China

Key Laboratory for Laser Plasma (Ministry of Education), Collaborative Innovation Center of IFSA (CICIFSA), Shanghai Jiao Tong University 800 Dongchuan Road, Shanghai 200240, P. R. China

**xfchen@sjtu.edu.cn*

Received 5 August 2017
Accepted 16 October 2017
Published 9 November 2017

We numerically and experimentally investigated the Cherenkov-type second harmonic generation of structured fundamental wave, whose phase was periodically modulated, in periodically poled nonlinear crystals. The Cherenkov-type second harmonic generation with different parameters of the structured fundamental wave was investigated. The experimental results are in good agreement with the theoretical analysis. This study provides a method of dynamically tailoring the Cherenkov-type second harmonic wave and also has potential application in other nonlinear frequency conversion processes.

Keywords: Nonlinear optics; computer holography; harmonic generation and mixing.

1. Introduction

Nonlinear Cherenkov radiation (NCR) has been extensively studied in nonlinear optics.[1–4] It is the extension of the conventional Cherenkov radiation (CR) in which the coherent light can be emitted when a charged particle travels faster than the speed of light in a medium, in the field of nonlinear optics. Similarly, in the case of NCR, it occurs when the phase velocity ν of the fundamental wave (FW) surpasses the harmonic radiation's phase velocity ν' in a nonlinear optical crystal.[5] In the second harmonic (SH) process, SH signal can be radiated at an angle defined by the longitudinal phase-matching condition $\cos\theta = \nu'/\nu = 2|k_1|/|k_2|$, with θ denoting the emission angle of NCR, k_1, k_2 being wave vectors of FW and SH waves, respectively.[6] Early works have reported NCR in a thin-film waveguide.[7] While with the concept of

*Corresponding author.

quasi-phase-matching (QPM) brought forward, it has been shown that this type of NCR is easier to observe in nonlinear photonic crystals (NPCs) with spatial modulation of the second-order susceptibility $\chi^{(2)}$.[8–11] In previous researches, controlling the emission properties of SH signals had drawn lots of attention. There were mainly two methods to tailor the emission of NCR, e.g., by means of designing the structure of NPCs or manipulating the incident FW. In the first method, the Cherenkov-type SH emission was first reported in one-dimensional (1D) NPCs.[9] Then, several publications reported on the Cherenkov-type SH emission in different types of 2D NPCs, such as rectangular, annularly, decagonal, and partially or totally disordered poled structures.[10–12] The theoretical systematic analysis of tailoring Cherenkov-type SH in 2D NPCs with longitudinal modulation of the second-order susceptibility $\chi^{(2)}$ was given in Ref. 13. In addition, the intensity enhancement of NCR at the interface of two different nonlinear media was experimentally demonstrated.[14–18] However, this method encounters some restrictions and inflexibility due to technical difficulties in fabricating artificial structures and unchangeable SH patterns. Hence, an alternative method paid attention to manipulating the FW incident. For instance, the Cherenkov-type SH emission could be dramatically enhanced by tuning the incident angle of the FW.[19,20] The intensity of the Cherenkov-type SH ring in the azimuthal direction could be modulated by varying the polarization of the FW.[21,22] It has been shown that changing the beam width of the incident beam not only affects the strength of NCR but also changes the sensitivity of the emission process to wavelength tuning.[23] Furthermore, the Cherenkov-type SH was also influenced by beam position, wavelength, and so on.[24] However, in these works, the attention was only paid on some simple parameters, which also limit the controllability of the Cherenkov-type SH wave.

In our previous researches, the concept of structured FW,[25–28] whose phase structure was periodically or randomly modulated by a spatial light modulation (SLM) in real time, was introduced into nonlinear frequency conversion processes. In this scheme, more degrees of freedom of the FW can be manipulated. This is crucial for the SH shaping and it would also be more flexible for controlling the Cherenkov-type SH emission.

In this paper, we numerically and experimentally investigated the Cherenkov-type SH generation of structured FW, whose phase was periodically modulated, in periodically poled nonlinear crystals. As shown in Fig. 1, NPC was modulated along x-axis, the FW was modulated along an angel θ with x-axis, and the reciprocal vector direction provided by NPC and the FW was $\mathbf{G}_k$ and $\mathbf{G}_m$, respectively. In case of $\theta = 90°$, the Cherenkov-type SH signal split into different orders. The odd-order Cherenkov-type SH disappeared when $\phi = \pi$ and the duty cycle $D = 0.5$. In case of $\theta = 0°$, the length along x-axis of the strip-shaped Cherenkov-type SH was longer than the case of without phase modulation of the FW. Moreover, with the changing of θ, different orders of the strip-shaped Cherenkov-type SH on the screen were always arranged along the direction of $\mathbf{G}_m$.

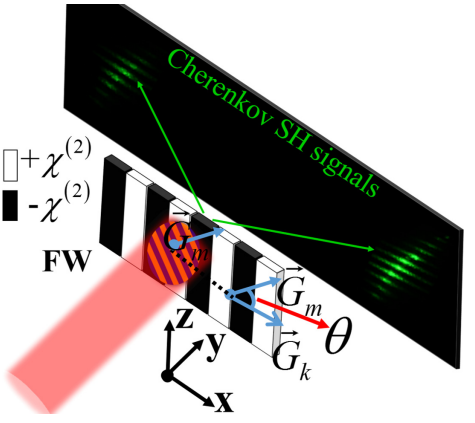

Fig. 1. Schematic of the experimental setup. The extraordinarily polarized FW with phase periodical modulated from 0 to ϕ propagates along y-axis of a periodical poled NPC, and the emitted Cherenkov-type SH pattern is projected onto a screen behind the crystal.

2. The Theoretical Analysis

The FW propagates along y-axis of the nonlinear crystal, as shown in Fig. 1. Without phase modulation, the FW can be defined as $\mathbf{E}_1 = A_1 e^{-i(\mathbf{k}_1 y - \omega t)}$, where A_1 and $\mathbf{k_1}$ are the maximum pump amplitudes at the center and wave vector of the FW, respectively. When the phase of the FW is periodically modulated, under the nondiffraction assumption, the FW can be described as an expansion of Fourier series:

$$\mathbf{E}_1 = A_1(x,z) \sum_{m=-\infty}^{+\infty} C_m e^{-i\mathbf{G}_m \cdot \mathbf{r}} e^{-i(\mathbf{k}_1 y - \omega t)}, \tag{2.1}$$

where $A_1(x,z)$ is the amplitude of the fundamental field and for a Gaussian beam it reads $A_1(x,z) = A_1 e^{-(x^2+z^2)/a^2}$ with a being beam diameter. C_m and $|\mathbf{G}_\mathrm{m}| = 2\pi\mathrm{m}/\Lambda$ (Λ is the modulated period of the FW) denote the Fourier coefficients and the reciprocal vectors of the FW, respectively. $\mathbf{r} = \mathbf{x}\cos\theta + \mathbf{z}\sin\theta$ is the transverse coordinate, θ is the angle between $\mathbf{G}_m$ and $\mathbf{G}_k$, as illustrated in Fig. 1. If the phase of the incident FW is periodically modulated from 0 to ϕ and the duty cycle D is 0.5, which is defined by the ratio of the length of the phase with ϕ to the entire period of the phase modulated structure, the Fourier coefficients are $C_0 = \frac{1}{2}(1 + e^{i\phi})$ and $C_m = \frac{i[\cos(m\pi)-1]}{2m\pi}(1 - e^{i\phi})$.[28]

Under the undepleted pump approximation of the FW and slowly varying envelop of the SH wave, the amplitude of the SH can be governed by the coupled wave equation:

$$\left(\frac{\partial}{\partial y} + \frac{i}{2k_2}\frac{\partial^2}{\partial x^2} + \frac{i}{2k_2}\frac{\partial^2}{\partial z^2}\right) A_2(x,y,z)$$
$$= -ig(x)\beta_2 {A_1}^2(x,z) e^{i\Delta k y} \times \left[\sum_{m=-\infty}^{+\infty} C_m e^{-i\mathbf{G}_m \cdot (\mathbf{x}\cos\theta + \mathbf{z}\sin\theta)}\right]^2, \tag{2.2}$$

where $\Delta k = k_2 - 2k_1$ is the wave vector mismatch between the SH wave and FW, $g(x)$ is the function characterizing the spatial distribution of the $\chi^{(2)}$. For a periodically poled NPC, it can be represented as a Fourier series: $g(x) = \sum_{k=-\infty}^{+\infty} g_k e^{i\mathbf{G}_k x}$, where g_k represents the Fourier coefficients of the crystal structure. In this case, $g_k(k \neq 0) = 2\sin(\pi k D)/\pi k$ and $g_0 = 2D - 1$ with the duty cycle D of the NPC defined by the ratio of the length of the positive domains to the entire period of the $\chi^{(2)}$ structure. $\beta_2 = k_2\chi^{(2)}/(2n_2^2)$ is the nonlinear coupling coefficient, with n_2 being the refractive index of the SH.

In order to figure out Eq. (2.2), we represent the amplitude through the 2D Fourier spectrum:

$$A_2(k_x, y, k_z) = \int A_2(x, y, z) e^{ik_x x} e^{ik_z z} dx dz, \tag{2.3}$$

where k_x, k_z are wave vectors of the FW along the x-axis and z-axis, respectively.

By substituting Eq. (2.3) into Eq. (2.2), we can obtain

$$\begin{aligned}\left(\frac{\partial}{\partial y} - \frac{i({k_x}^2 + {k_z}^2)}{2k_2}\right) A_2(k_x, y, k_z) \\ = -i\beta_2 e^{i\Delta k y} \times \int {A_1}^2(x, z) g(x) \left[\sum_{m=-\infty}^{+\infty} C_m e^{-i\mathbf{G}_m \cdot (\mathbf{x}\cos\theta + \mathbf{z}\sin\theta)}\right]^2 \\ \times e^{ik_x x} e^{ik_z z} dx dz.\end{aligned} \tag{2.4}$$

Then, the amplitude of the SH can be expressed as

$$\begin{aligned}A_2(k_x, y, k_z) = -iy\beta_2 e^{i\left(\Delta k + \frac{{k_x}^2 + {k_z}^2}{2k_2}\right) y} \sin c^2\left[\left(\Delta k - \frac{{k_x}^2 + {k_z}^2}{2k_2}\right) y \Big/ 2\right] \\ \times \int {A_1}^2(x, z) g(x) \left[\sum_{m=-\infty}^{+\infty} C_m e^{-i\mathbf{G}_m \cdot (\mathbf{x}\cos\theta + \mathbf{z}\sin\theta)}\right]^2 e^{ik_x x} e^{ik_z z} dx dz,\end{aligned} \tag{2.5}$$

where y is the interaction distance of the nonlinear process.

Finally, integral in Eq. (2.5) and considering the spectral density of the SH $I_2(k_x, y, k_z) = |A_2(k_x, y, k_z)|^2$, we have the following expression:

$$\begin{aligned}I_2(k_x, y, k_z) = \left(\frac{\pi}{2} a^2 \beta_2 y {A_1}^2\right)^2 \sin c^2\left[\left(\Delta k - \frac{{k_x}^2 + {k_z}^2}{2k_2}\right) y \Big/ 2\right] \\ \times \left[b_q \sum_{k=-\infty}^{+\infty} g_k \sum_{q=-\infty}^{+\infty} e^{-\frac{a^2}{8}(G_k + k_x - G_q\cos\theta)^2} e^{-\frac{a^2}{8}(k_z - G_q\sin\theta)^2}\right]^2\end{aligned} \tag{2.6}$$

with $b_q = \sum_{m,n}^{m+n=q} |C_m C_n| (q = m + n)$ being the Fourier coefficients of the SH and the summation from $-\infty$ to $+\infty, G_q = G_m + G_n$.

3. Experimental Results and Discussion

In our experiment, the FW was delivered from a mock-locked Nd:YAG nanosecond laser with the wavelength at 1064 nm. The phase structure of the FW was modulated by an SLM and it has a resolution of 1920 × 1080 pixels. After the SLM, the FW was imaged by a 4-f system to imprint the structured FW to the onset of a periodically poled crystal. Without loss of generality, periodically poled $LiNbO_3$ (PPLN) fabricated by electric field poling technique was used in the experiment at the room temperature. The size of the PPLN was 11.0 mm $(x) \times 0.5$ mm $(y) \times 1.0$ mm (z) and the duty cycle $D = 0.5$. The period Λ of the PPLN was 10 μm. The FW was kept as e-polarized and propagated along y-axis of PPLN, as shown in Fig. 1. The type of the Cherenkov-type SH generation process is $e_1 e_1 - e_2$. According to the Sellmeier equation, $n_1 = 2.1483$ and $n_2 = 2.2246$. The beam diameter a at the input facet of the sample was about 2 mm. After the PPLN, the FW was filtered out by a short-pass filter and the Cherenkov-type SH wave was projected on a screen located 13 cm behind the crystal. Finally, the SH pattern was captured by a camera.

In order to illustrate the different SH phenomenon caused by phase modulation of the FW, we did a comparative experiment. First, without phase modulation of the FW, as shown in Fig. 2(a), the simulated and experimental results are shown in Figs. 2(b) and 2(c), respectively. The Cherenkov-type SH exhibits as a symmetric strip-shaped distribution with respect to the propagation direction of the FW. However, in the experiment, the longer Cherenkov-type SH signal is caused by the thickness of the crystal, the position of screen after the PPLN, and the imperfect domain wall structure of the PPLN. The corresponding external angle of the Cherenkov-type SH is $\pm 35^\circ$ in the experiment. This is in good agreement with the theoretical prediction ($\beta = \sin^{-1}\{n_2 \sin[\cos^{-1}(2k_1/k_2)]\} = \pm 35.3^\circ$).

Second, the phase of the FW was periodically modulated from 0 to $\pi/2$ with the duty cycle $D = 0.5, \theta = 90^\circ$, and the modulated period of the FW $\Lambda = 65\mu$ m, respectively. The phase structure of the FW is shown in Fig. 2(d). In this case, the previous strip-shaped Cherenkov-type SH in each side is split into different orders. The simulated result is shown in Fig. 2(e). As can be seen from the experimental result shown in Fig. 2(f), 0 to 8-order of the strip-shaped Cherenkov-type SH can be observed. The intensity of the different orders Cherenkov-type SH is proportional to the Fourier coefficients $b_q = \sum_{m,n}^{m+n=q} |C_m C_n|$. In this situation, each order of b_q is nonzero and higher order Cherenkov-type SH signals are not observed owing to smaller Fourier coefficients b_q, which also leads to the shorter strip-shaped Cherenkov-type SH. Besides, the relative distance between different orders strip-shaped Cherenkov-type SH is increasing with decreasing of the modulated period of the FW, which can be observed in the experiments.

Next, the Cherenkov-type SH was observed with changing parameter ϕ. From the Fourier coefficient of $C_0 = \frac{1}{2}(1 + e^{i\phi})$ and $C_m = \frac{i[\cos(m\pi)-1]}{2m\pi}(1 - e^{i\phi})$, the value of ϕ determines the relative values of C_m. According to Eq. (2.6), the intensity of the Cherenkov-type SH $I_2 \propto {b_q}^2 (b_q = \sum_{m,n}^{m+n=q} |C_m C_n|)$. Hence, the value of ϕ influences

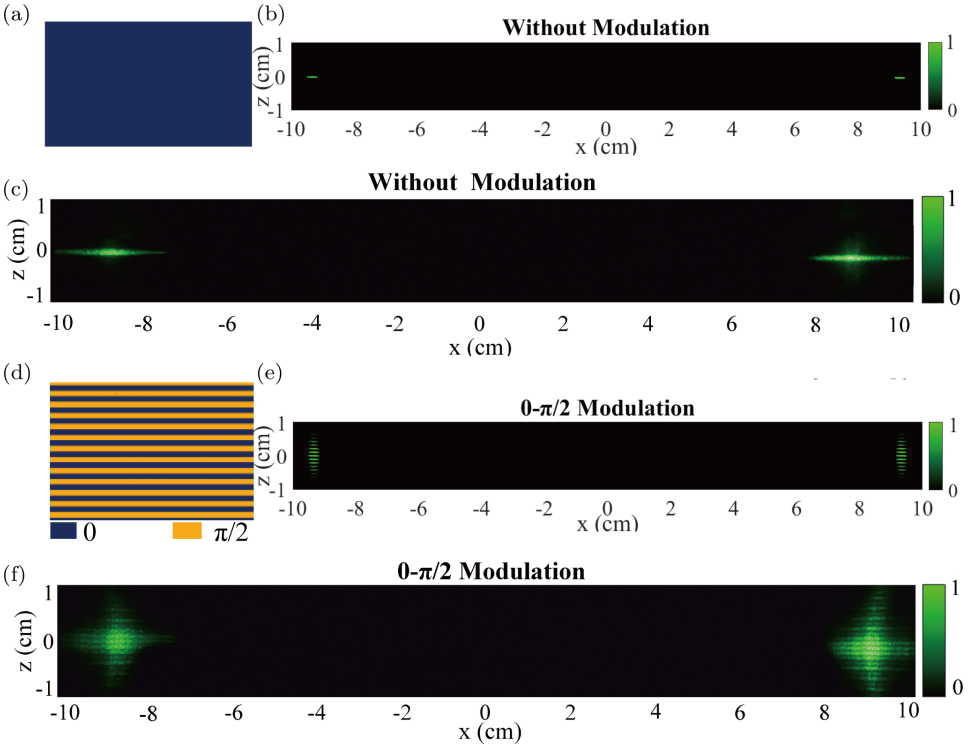

Fig. 2. (a) The structure of the FW without phase modulation. (b) and (c) The simulated and experimental results of the Cherenkov-type SH corresponding to (a). (d) The phase structure of the FW modulated from 0 to $\pi/2$ with $\Lambda = 65\mu$m and $D = 0.5$. (e) and (f) The simulated and experimental results of the Cherenkov-type SH corresponding to (d).

the relative intensity of the different orders Cherenkov-type SH. However, the interesting phenomenon is observed when $\phi = \pi$. Figure 3(a) represents the phase structure of the FW with the duty cycle $D = 0.5, \theta = 90^\circ$ and $\Lambda = 65\mu$m. In this case, odd-orders strip-shaped Cherenkov-type SH disappeared. Compared with the case of $\phi = \pi/2$ in Figs. 2(e) and 2(f), the corresponding simulated and experimental results displayed in Figs. 3(b) and 3(c) clearly show that the odd-ordered strip-shaped Cherenkov-type SH was not observed. This phenomenon is similar to the nonlinear Raman–Nath SH generation analyzed in Ref. 28, which was caused by $b_q = \sum_{m,n}^{m+n=q} |C_m C_n| = 0$ (the value of C_m is 0 if m is even) for the odd-orders of the Cherenkov-type SH.

Then, the structure of the FW was periodically sharply modulated from 0 to $\pi/2$ and $\theta = 0^\circ$, as shown in Fig. 4(a). The simulated and experimental results are shown in Figs. 4(b) and 4(c), respectively. Figures 4(d) and 4(e) show the profile of the Cherenkov-type SH along x-direction corresponding to the FW of Figs. 2(a) and 4(a), respectively. In Fig. 4(d), the full width at half maximum (FWHM) of the

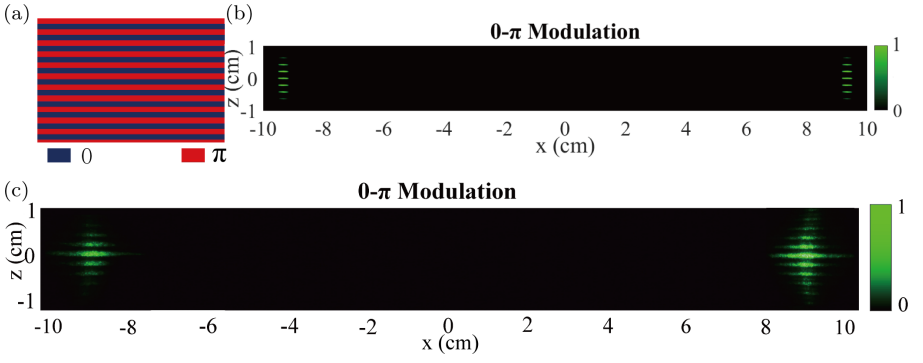

Fig. 3. (a) The structured FW modulated from 0 to π with $\Lambda = 65\mu$m and $D = 0.5$. (b) The simulated result of the Cherenkov-type SH corresponding to (a). (c) The experimental result of the Cherenkov-type SH corresponding to (a).

Cherenkov-type SH is 0.50 cm and 0.13 cm in experiment and theoretical calculation, respectively. When the phase of FW was periodically modulated from 0 to $\pi/2$, the FWHM of the Cherenkov-type SH is 0.66 cm and 0.16 cm in experiment and theoretical calculation, respectively. Compared with Fig. 2(d), in which the phase of the

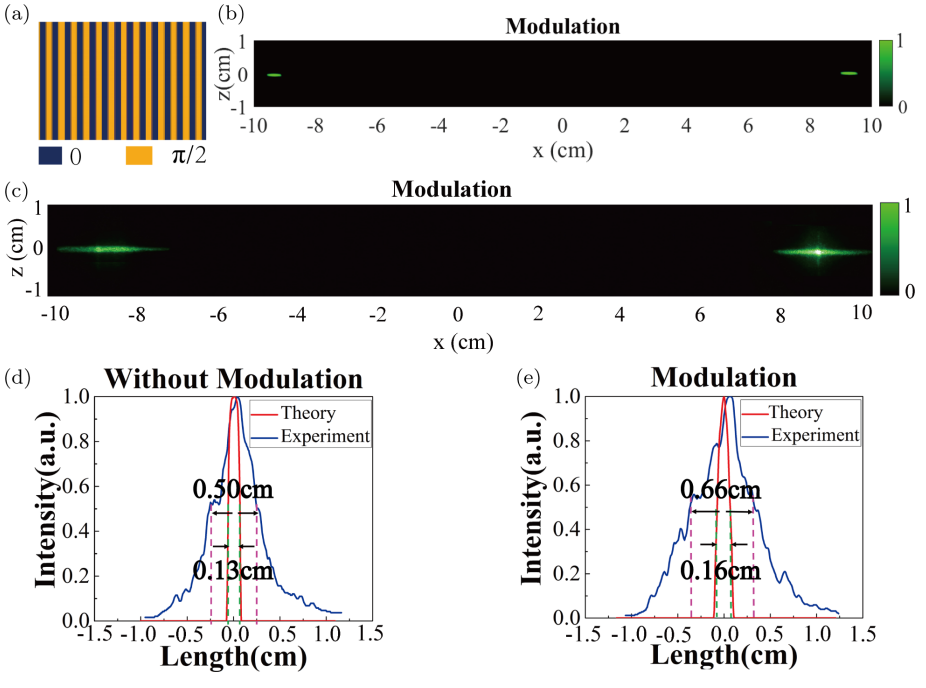

Fig. 4. (a) The phase structure of the FW modulated from 0 to $\pi/2$ with $\Lambda = 65\,\mu$m and $D = 0.5$. (b) and (c) The simulated and experimental results of the Cherenkov-type SH corresponding to (a). (d) The profile of the Cherenkov-type SH along x-direction without phase modulation of the FW. (e) The profile of the Cherenkov-type SH along x-direction corresponding to (a).

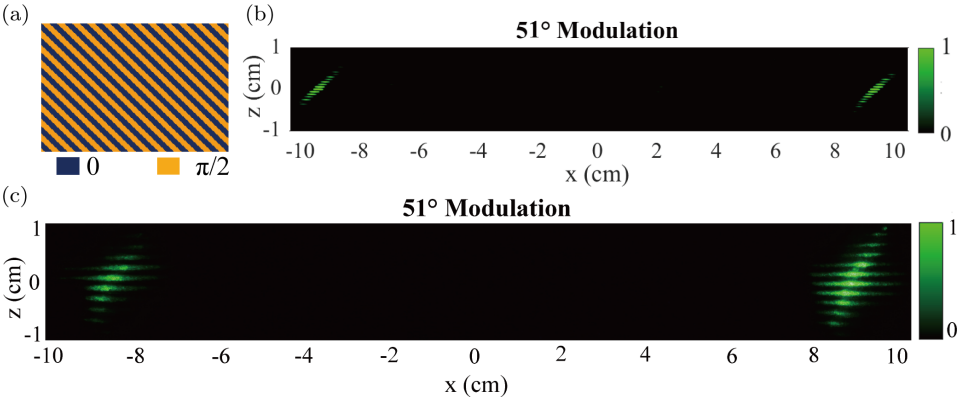

Fig. 5. (a) The phase structure of the FW with $\phi = \pi/2$ and $\theta = 51°$. (b) The simulated result of the Cherenkov-type SH corresponding to (a). (c) The experimental result of the Cherenkov-type SH corresponding to (a).

FW is not modulated, the strip-shaped Cherenkov-type SH shown in Fig. 4(e) is longer. This phenomenon is caused by the additional structure of the FW.

Furthermore, the Cherenkov-type SH was observed with θ changing. We find that different orders of the strip-shaped Cherenkov SH on the screen were always arranged along the direction of $\mathbf{G}_m$. Without loss the generality, we show the case of $\theta = 51°$. The phase of the FW is periodically modulated from 0 to $\pi/2$ and the period 90 μm, as illustrated in Fig. 5(a). In Fig. 5(b), the theoretical result shows different orders of Cherenkov-type SH arranged along 51° with respect to the x-direction in the screen plane. In the experiment shown in Fig. 5(c), such angle is 51.06°.

This study provides a way of dynamically tailoring the Cherenkov-type SH wave. Compared to the $\chi^{(2)}$ modulation, it is more flexible to modulate the FW itself because this method does not require complex sample fabrication procedures. The FW can be controlled by an SLM in real time, whereas SH generation in NPCs is fundamentally restricted by their predesigned structures. In contrast to other researches of changing some simple parameters of the incident FW (such as beam waist, polarization, position, incident angle, and so on), we introduced the concept of structured FW into tailoring the Cherenkov-type SH emission process. By this way, more degrees of freedom of the FW can be controlled and this is of great practical importance for the Cherenkov-type SH shaping.

4. Conclusion

In conclusion, we numerically and experimentally investigated the Cherenkov-type SH generation of the structured FW, whose phase was periodically modulated, in periodically poled nonlinear crystals. In case of $\theta = 90°$, the Cherenkov-type SH split into different orders. The odd-orders Cherenkov-type SH disappeared when $\phi = \pi, D = 0.5$. In case of $\theta = 0°$, the strip-shaped Cherenkov-type SH was longer

than the case of without phase modulation of the FW. Moreover, with changing of θ, different orders of the strip-shaped Cherenkov SH on the screen were always arranged along the direction of $\mathbf{G}_m$. Experimental results are in a good correspondence with the theoretical analysis. This study provides a method of dynamically tailoring the Cherenkov-type SH wave and also has potential application in other nonlinear frequency conversion processes.

Acknowledgment

This work was supported in part by the National Natural Science Foundation of China (NSFC) (61235009).

References

1. X. Deng, H. Ren, H. Lao and X. Chen, Research on Cherenkov second-harmonic generation in periodically poled lithium niobate by femtosecond pulse, *J. Opt. Soc. Am. B* **27**(7) (2010) 1475–1480.
2. V. Roppo, K. Kalinowski and Y. Sheng, Unified approach to Cerenkov second harmonic generation, *Opt. Exp.* **21**(22) (2013) 25715–25726.
3. V. Vaicaitis, Cherenkov-type phase matching in bulk KDP crystal, *Opt. Commun.* **209**(4) (2002) 485–490.
4. P. Lukin, I. Batkin, A. N. Almaliev, T. A. Churakova, M. A. Dolgopolov and I. V. Kopytin, Cherenkov radiation from electrons passing through human tissue, *J. Innov. Opt. Health Sci.* **10**(01) (2017) 1650055-1–1650055-5.
5. N. An, Y. Zheng, H. Ren, X. Zhao, X. Deng and X. Chen, Normal, degenerated, and anomalous-dispersion-like Cerenkov Sum-frequency generation in one nonlinear medium, *Photon. Res.* **3**(4) (2015) 106–109.
6. A. Shapira and A. Arie, Phase-matched nonlinear diffraction, *Opt. Lett.* **30**(10) (2011) 1933–1935.
7. P. Tien, R. Ulrich and R. Matin, Optical second harmonic generation in form of coherent Cherenkov radiation from a thin-film waveguide, *Appl. Phys. Lett.* **17**(10) (2008) 447–450.
8. Y. Sheng, W. Wang, R. Shiloh, V. Roppo, Y. Kong, A. Arie and W. Krolikowski, Cerenkov third-harmonic generation in nonlinear $\chi^{(2)}$ photonic crystal, *Appl. Phys. Lett.* **98**(24) (2011) 241114.
9. S. M. Saltiel, D. N. Neshev, W. Krolikowski, A. Arie, O. Bang and Y. S. Kivshar, Multiorder nonlinear diffraction in frequency doubling processes, *Opt. Lett.* **34**(6) (2009) 1699–1713.
10. W. Wang, Y. Sheng, Y. Kong, A. Arie and K. Kalinowski, Multiple Cerenkov second-harmonic waves in a two-dimensional nonlinear photonic structure. *Opt. Lett.* **35**(22) (2010) 3790–3792.
11. X. Wang, X. Zhao, Y. Zheng and X. Chen, Theoretical study on second-harmonic generation in two-dimensional nonlinear photonic crystals. *Appl. Opt.* **56**(3) (2017) 750–754.
12. Y. Sheng, V. Roppo and M. Ren, Multi-directional Cerenkov second harmonic generation in two-dimensional nonlinear photonic crystal, *Opt. Exp.* **20**(4) (2012) 3948–3950.
13. Y. Sheng, V. Roppo, Q. Kong, K. Kalinowski, Q. Wang, C. Cojocaru, J. Trull and W. Krolikowski, Tailoring Cerenkov second-harmonic generation in bulk nonlinear photonic crystal, *Opt. Lett.* **36**(13) (2011) 2593–2595.

14. X. Zhao, Y. Zheng, H. Ren, N. An, X. Deng and X. Chen, Nonlinear Cherenkov radiation at the interface of two different nonlinear media, *Opt. Exp.* **24**(12) (2016) 12825–12830.
15. H. Ren, X. Deng, Y. Zheng, N. An and X. Chen, Enhanced nonlinear Cherenkov radiation on the crystal boundary, *Opt. Lett.* **38**(11) (2013) 1993–1995.
16. Y. Sheng, V. Roppo, K. Kalinowski and W. Krolikowski, Role of a localized modulation of $\chi^{(2)}$ in Cerenkov second-harmonic generation in nonlinear bulk medium, *Opt. Lett.* **37**(18) (2012) 3864–3866.
17. X. Zhao, Y. Zheng, N. An, X. Deng, H. Ren and X. Chen, Surface enhanced nonlinear Cherenkov radiation in one-dimensional nonlinear photonic crystal, *Opt. Exp.* **25**(12) (2017) 13897–13902.
18. H. Ren, X. Deng, Y. Zheng and X. Chen, Single domain wall effect on parametric processes via Cherenkov-type phase matching, *J. Nonlinear Opt. Phys. Mater.* **20**(04) (2011) 459–466.
19. S. M. Saltiel, D. N. Neshevb, W. Krolikowskib, A. Ariec and Y. S. Kivsharb, Multi-conical second harmonic waves via nonlinear diffractions in circularly poled nonlinear media, *Proc. SPIE* **702**(723) (2008) 133–137.
20. K. Kalinowski, P. Roedig, Y. Sheng, M. Ayoub, J. Imbrock, C. Denz and W. Krolikowski, Enhanced Cerenkov second-harmonic emission in nonlinear photonic structures, *Opt. Lett.* **37**(11) (2012) 1832–1834.
21. Y. Sheng, S. M. Saltiel, W. Krolikowski, A. Arie, K. Koynov and Y. S. Kivshar, Cerenkov-type second-harmonic generation with fundamental beams of different polarizations, *Opt. Lett.* **35**(9) (2010) 1317–1319.
22. S. M. Saltiel, D. N. Neshev, R. Fischer, W. Krolikowski, A. Arie and Y. S. Kivshar, Generation of second-harmonic conical waves via nonlinear bragg diffraction, *Phys. Rev. Lett.* **100**(10) (2008) 103902-1–103902-4.
23. Y. Sheng, Q. Kong, V. Roppo, K. Kalinowski, Q. Wang, C. Cojocaru and W. Krolikowski, Theoretical study of Cerenkov-type second-harmonic generation in periodically poled ferroelectric crystals, *J. Opt. Soc. Am. B* **29**(3) (2012) 312–314.
24. K. Kalinowski, Q. Kong, V. Roppo, A. Arie, Y. Sheng and W. Krolikowski, Wavelength and position tuning of Cerenkov second-harmonic generation in optical superlattice, *Appl. Phys. Lett.* **99** (2011) 181128-1–181128-3.
25. A. Shapira, L. Naor and A. Arie, Nonlinear optical holograms for spatial and spectral shaping of light waves, *Sci. Bull.* **60**(16) (2015) 1403–1415.
26. A. Shapira, R. Shiloh, I. Juwiler and A. Arie, Two-dimensional nonlinear beam shaping, *Opt. Lett.* **37**(11) (2012) 2136–2138.
27. H. Zhou, H. Liu, M. Sang, J. Li and X. Chen, Nonlinear Raman-Nath second harmonic generation of hybrid structured fundamental wave, *Opt. Exp.* **25**(4) (2017) 3774–3779.
28. H. Liu, J. Li, X. Zhao, Y. Zheng and X. Chen, Nonlinear Raman-Nath second harmonic generation with structured fundamental wave, *Opt. Exp.* **24**(11) (2016) 15666–15671.